Three-Dimensional Rotational Myelography

Markus Kufeld, Benjamin Claus, Adriana Campi, Wolfgang R. Lanksch and Goetz Benndorf

AJNR Am J Neuroradiol 2003, 24 (7) 1290-1293
http://www.ajnr.org/content/24/7/1290

AJNR Am J Neuroradiol 24:1290–1293, August 2003

Technical Note

Three-Dimensional Rotational Myelography

Markus Kufeld, Benjamin Claus, Adriana Campi, Wolfgang R. Lanksch, and Goetz Benndorf

Summary: Three-dimensional (3D) rotational radiography, initially developed to visualize intracranial aneurysms, is applied to the cervical spine after conventional myelography. We call this process *3D rotational myelography*. 3D reconstruction and then postprocessing allows imaging in multiple planes. Spinal or nerve root sheath alterations caused by bony or soft tissue can be visualized and differentiated by using this technique.

Rotational angiography of intracranial vessels was described and clinically applied by Voigt et al (1) in 1975. Diagnostic applications and technical improvements of rotational digital subtraction angiography were reported by Schumacher et al (2) in 1989. Although developed for intracranial vascular imaging (especially imaging of aneurysms), this method can be applied to other diagnostic tests. We produced digital rotational radiographs after obtaining conventional cervical myelograms to apply the advantage of 3D rotational myelography and image postprocessing to spinal imaging.

Technique

After performing conventional cervical myelography, rotational radiographs are obtained on a commercial digital biplane angiography system (Neurostar Top, Siemens). A 200-degree rotation forward and backward of the tube-camera unit around the patient's longitudinal axis within 14 seconds is performed by using an acquisition matrix of 1024 × 1024 pixels. The forth and back rotation results in 124 radiographs. Raw data are transferred via local area network to a graphic workstation (Siemens 3DVirtuoso), where the rotational projection images are prepared for computed 3D reconstruction. 2D radiographs are used to determine the volume of interest. After correction of gain and distortion, a 3D data set is calculated, resulting in 512 transverse CT-equivalent sections. Depending on the initially chosen volume of interest, the voxel size varies from 0.1 to 0.6 mm. We used a resolution of 0.14-mm voxel size, which resulted in a 3D cuboid of 7.16 × 7.16 × 14.34 cm. Reconstruction time was 15 minutes. Detailed information regarding technical performance and reconstruction procedure has been reported (3). Postprocessing techniques provided by the software included real-time 3D volume rendering and multiplanar reformatting. Real-time 3D volume rendering creates a 3D model of the examined object. The software allows emphasizing bony structures or soft tissue by changing intensity, brightness, and opacity of different X-ray structures. Additionally, rotation of the 3D object in all directions is possible, as is a virtual stereoscopic view provided by the software in combination with special glasses. The multiplanar reformatting modus generates virtual sections according to the three main axes and free defined axes. The section planes can be freely chosen, and curved sectioning is also possible. By tilting the section planes corresponding to the nerve root channel, an exact orthogonal section series along the nerve root sheath can be produced.

Received November 25, 2002; accepted after revision March 14, 2003.

From the Departments of Neurosurgery (M.K., W.R. L.) and Radiology (B.C., G.B.), Humboldt University Charité, Berlin, Germany, and the Department of Neuroradiology (A.C.), University Hospital Zurich, Zurich, Switzerland.

Address reprint requests to Goetz Benndorf, Department of Neurosurgery, Charité Campus Virchow Klinikum, Augustenburger Platz 1, 13353 Berlin, Germany.

Case Report

A 60-year-old man presented with severe cervicobrachialgia and dysesthesia on the right side, which were confirmed by electromyography that revealed a right-sided C6 radicular syndrome; the results of CT, however, were indefinite. Cervical myelograms, obtained via C1–C2 puncture and injection of 20 mL of Isovist 300 (Schering), showed slight compression of the whole spinal cord and well-distinguishable defects of the contrast column according to the right-sided nerve root sheaths of C6 and C7 and a major filling defect of the right C6 root sheath (Fig 1A and B). Without superimposing structures, 3D rotational myelography allowed, in different planes, clearer visualization of the thecal sac and the dural root sleeves. By image postprocessing with real-time 3D (Fig 2) and multiplanar reformatting (Figs 3 and 4), the compression of the right C6 nerve root was revealed as explanation for the clinical symptoms. Transversal (axial) sections showed a large mediolateral compression of the nerve root sheath by a mostly soft tissue protrusion from the disk space C5–C6 (Fig 4A, *inset*). After foraminotomy at level C5–C6 on the right side and extraction of small disk sequesters and bony resection, the patient reported satisfying pain relief, which confirmed the diagnosis of a right-sided disk protrusion and osteochondrosis with foraminal stenosis at disk space level C5–C6.

Discussion

We successfully applied the technique of 3D rotational radiography to cervical myelography. In addition to standard myelographic views, we were able to visualize anatomic details, such as the thecal sac and the dural root sleeves, by image postprocessing after 3D reconstruction. The wide range of contrast sensitivity allowed differentiated characterization of bone versus soft tissue (disk) lesions (4).

Multiplanar reformatting allows the radiologist to easily and actively interact with images, obtaining coronal, axial, paraxial sagittal, and parasagittal reconstructions with different degrees of obliquity. This is important for adequate assessment of patients with scoliosis and for all patients whose clinical signs are not congruent with MR imaging or CT findings. Abnormal findings, such as intra- and extraforaminal disk herniations, osteophytes, or neoplastic lesions causing severe narrowing, which often are subtle be-

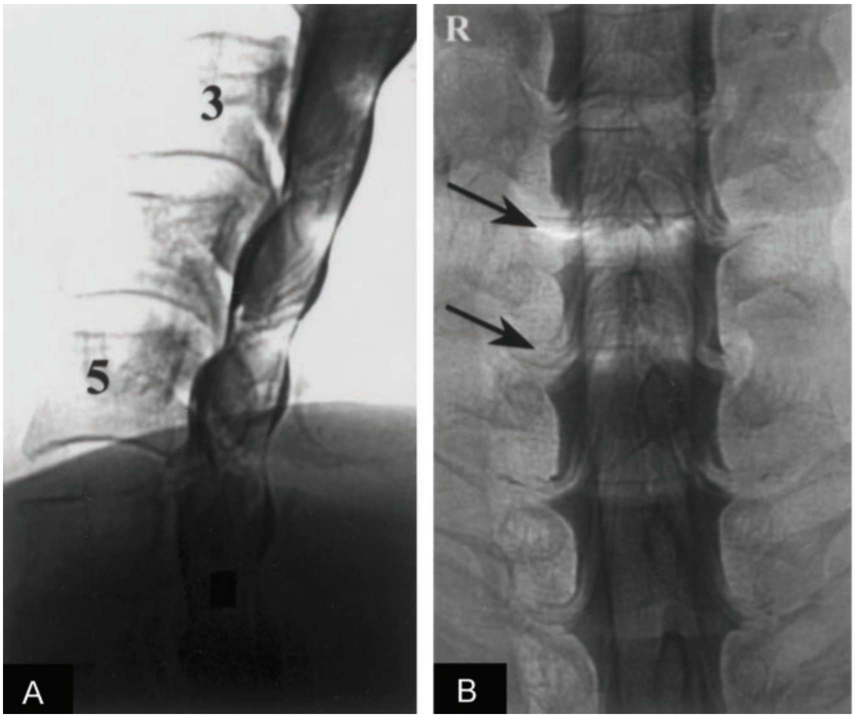

FIG 1. Images from the case of a 60-year-old man who presented with severe cervicobrachialgia and dysesthesia on the right side.

A, Lateral myelogram shows multiple anterior defects that indicate general narrowing of the spinal canal with ventral bony spurs and a steep vertebral column. At disk level C5–C6, an additional disk protrusion can only be assumed.

B, Anteroposterior myelogram shows right-sided local compression of root sleeves C6 and C7, with a major defect at C6 (*arrows*).

FIG 2. Real-time 3D reconstruction of cervical spine, with differentiation of the contrast column from bone, shows relationship between thecal sac and bony structures. This oblique projection, similar to a conventional myelogram, shows the filling defect in the neural foramen of C5–C6 (*arrow*), indicating major deficit at this level.

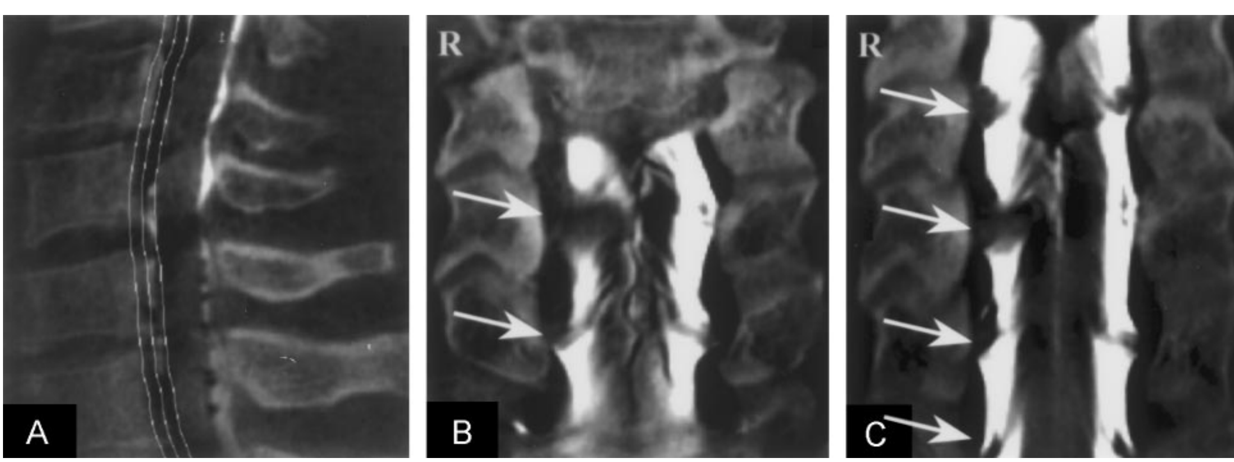

FIG 3. Coronal multiplanar reformatting.

A, Lateral reconstruction localizer in the multiplanar reformatting mode indicates coronal curved planes of reconstruction (see *C*), following the physiological lordosis of the spine.

B, Image shows multiplanar reformatting with coronal plane of reconstruction. This plane is straight and limits the visualization and comparison of the root sleeves. Because of the physiological lordosis of the cervical spine, the nerve root sheaths are mostly out of the cutting plane and thus are difficult to compare for evaluation of maximum nerve root compression (*arrows*).

C, Image shows reformatting with curved coronal planes of reconstruction, following the physiological lordosis of the spine. The visualization of several nerve root sheaths is possible in the same plane (*arrows*), allowing simultaneous assessment of multilevel abnormalities. By comparison, straight coronal plane multiplanar reformatting shows only two nerve roots sheaths (see *B*, *arrows*).

cause they are laterally located, can be better shown. With multiplanar reformatting, the nerve root sheath can be more peripherally followed and visualized. With CT and MR imaging, delineation of narrowing structures in this region usually proves to be difficult because of the oblique course of the bony nerve root channel in relationship to the standard axial or sagittal section plane (5). Furthermore, partial volume averaging and variable signal intensity of disk and bone spurs may disturb the image quality (6). Thus,

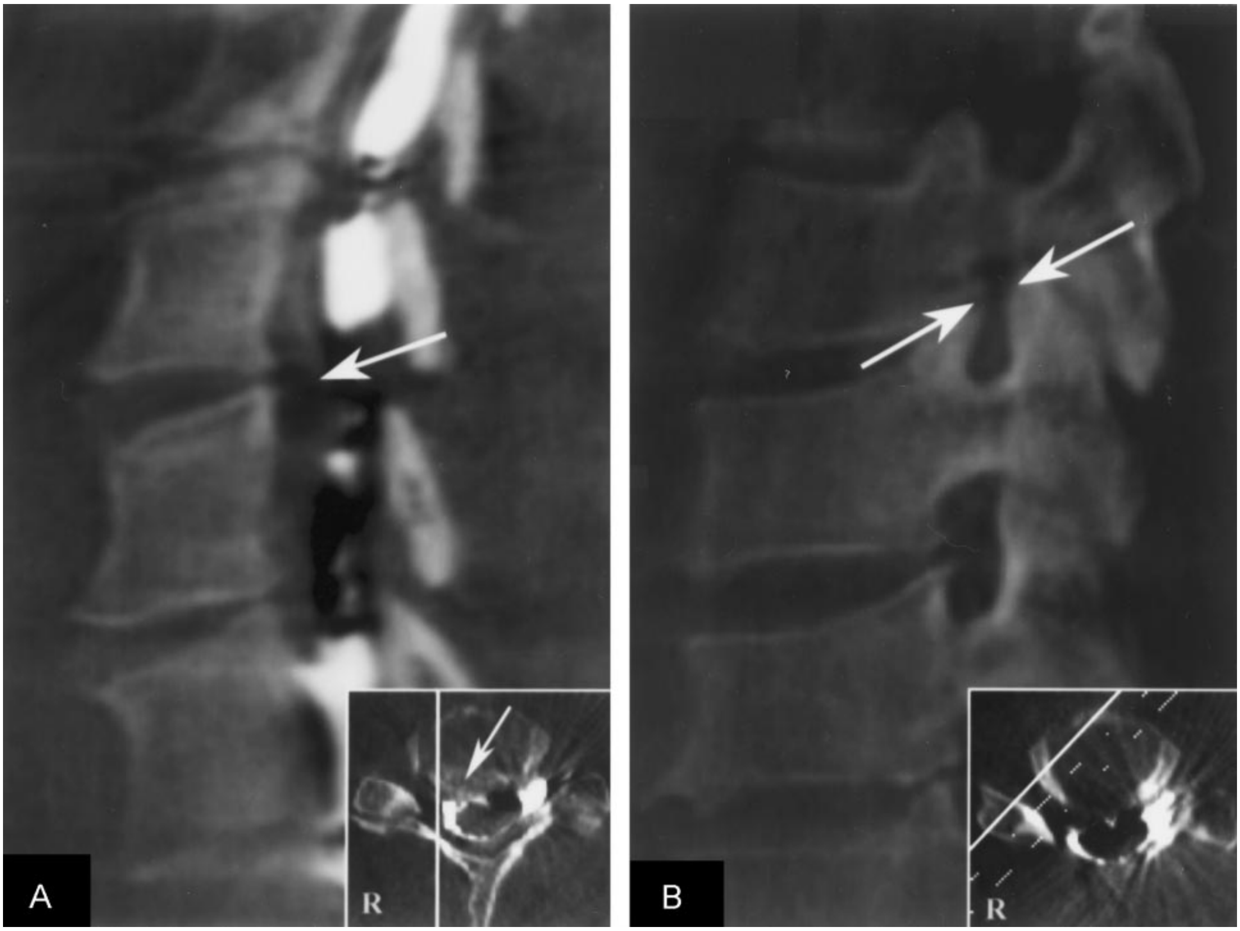

FIG 4. Parasagittal multiplanar reformatting.

A, Right-sided parasagittal reconstruction of the spine in multiplanar reformatting modus is shown. The defect of the contrast column at the C5–C6 level indicates nerve root sheath compression and also allows distinction between the compressing disk material and the vertebra (*arrow*). *Inset*, multiplanar reformatting with axial orientation of the reconstruction plane at the C5–C6 level shows a narrowing of the neural foramen on the right side. The contrast medium is asymmetrically distributed within the spinal canal, indicating a right paramedian soft disk protrusion with compression of the thecal sac and the spinal cord (*arrow*). *White line* marks reconstruction plane in relation to spinal canal.

B, Multiplanar reformatting in oblique parasagittal projection obtained perpendicular to the course of the nerve root canal allows assessment of narrowing of the foramen (*arrows*). As the *inset* in *A* shows (*white line* shows reconstruction plane), an evaluation of the neural foramen along its course is possible, allowing determination of maximum stenosis.

an additional view orientated perpendicular to the course of the neural foramina, as provided by multiplanar reformatting, may facilitate localization of laterally displaced nonossified disks and focal spurs in foraminal stenosis. This information can be essential for surgeons to decide whether anterior cervical diskectomy or dorsal foraminotomy is necessary.

Compared with CT myelography, 3D rotational myelography provides immediate rotational images and 3D reconstruction without transferring the patient to another imaging unit. It requires, however, a more attenuated contrast column than does CT myelography and has to be performed immediately after injection of intrathecal contrast material. 3D data obtained by using this technique based on a 1024 × 1024 matrix may be superior to CT myelography data according to detail resolution and 3D visualization. This is also supported by results recently published by El-Sheik et al (7), who performed studies on artificially produced bone fractures in pigs.

The main disadvantages of this technique compared with MR imaging, MR myelography, and CT myelography are inferior differentiation of various soft tissues (MR imaging), availability of equipment, dependence on a well-trained neuroradiologist (when performing C1–C2 puncture), sensitivity to motion artifacts (when using 14-s rotation), and adequate positioning of the patient. Invasiveness is the main drawback of 3D rotational myelography in comparison with MR imaging, but in cases in which myelography is being performed anyway, no additional puncture is necessary.

Conclusion

3D rotational myelography and image postprocessing provide a well-applicable technique that offers a valuable, time-efficient, diagnostic tool for the preoperative evaluation of cervical spinal lesions. Additional information to that obtained by standard myelography, CT, and MR imaging can easily be obtained in cases in which distinctive imaging information is needed. At our institution, this technique has therefore become a routine in cases in which cervical myelography (C1–C2 puncture) is performed; we have applied the technique to 22 cases thus far. Further studies are in progress to compare 3D rotational myelography with CT myelography, native CT, and MR imaging.

References

1. Voigt K, Stoeter P, Petersen D. **Rotational cerebral roentgenography: I. evaluation of the technical procedure and diagnostic application with model studies.** *Neuroradiology* 1975;10:95–100
2. Schumacher M, Kutluk K, Ott D. **Digital rotational radiography in neuroradiology.** *AJNR Am J Neuroradiol* 1989;10:644–649
3. Wiesent K, Barth K, Navab N, et al. **Enhanced 3-D-reconstruction algorithm for C-arm systems suitable for interventional procedures.** *IEEE Trans Med Imaging* 2000;19:391–403
4. Daniels DL, Grogan JP, Johansen JG, Meyer GA, Williams AL, Haughton VM. **Cervical radiculopathy: computed tomography and myelography compared.** *Radiology* 1984;151:109–113
5. Larsson EM, Holtas S, Cronqvist S, Brandt L. **Comparison of myelography, CT myelography and magnetic resonance imaging in cervical spondylosis and disk herniation: pre- and postoperative findings.** *Acta Radiol* 1989;30:233–239
6. Ji B, Wruck A. **Myelography and nuclear magnetic resonance imaging of the cervical syndrome [in German].** *Rontgenpraxis* 1998; 51:373–378
7. El-Sheik M, Heverhagen JT, Alfke H, et al. **Multiplanar reconstructions and three-dimensional imaging (computed rotational osteography) of complex fractures by using a C-arm system: initial results.** *Radiology* 2001;221:843–849